Pressure patches for membranes: The induced pinch of a grafted polymer

T. Bickel and C. Marques

LDFC-UMR 7506, 3 rue de l'Université, 67084 Strasbourg Cedex, France

C. Jeppesen

Materials Research Laboratory, University of California, Santa Barbara, California 93106

Achieving control of membrane shape and topology is of crucial importance to regulate function and performance of many systems in the realms of biology, physics, and chemical sciences. The design of a kit of versatile microscopic tools for tuning the shapes of fluid membranes relies ultimately on the possibility of tailoring molecules for applying a given, well-chosen force, to the self-assembled interfaces. Here we discuss theoretically the ability of grafted polymers to perform as mesoscopic pressure patches. We compute the pressure that a grafted polymer applies to the supporting surface. We also show that this entropic pressure leads to a well-defined pinched form of the membranes. Moreover, new membrane-mediated forces result from the action of these pressure tools, enabling action upon their spatial distribution along the membrane surface.

Membranes are pervasive constituents of biological and industrial suspensions. The walls of cells and liposomes are self-assembled fluid bilayers that not only circumscribe an inner space but also host a variety of macromolecular bodies performing different functions: coating protection, ion exchange, mechanical reinforcement, etc. [1]. Industrial formulations of cosmetics, pharmaceuticals, or detergents [2] are often membrane solutions, containing also macromolecules optimized for performance, processing, conditioning, or delivery. Recent studies have shown that added polymers or colloids can change the behavior of such membrane systems. Polymers grafted to the bilayers induce gelation [3] or other phase changes [4,5] in liquid lamellar phases, stabilize monodisperse vesicles [6] or modify the geometry of monolamellar [7,8] and multilamellar cylindrical vesicles [9].

We show in this paper that two fundamental forces come into play whenever non-adsorbing polymer chains are attached to a deformable surface. The first is a non-homogeneous pressure field applied by the polymer onto the membrane, due to the entropic repulsion between the surface and the polymer. Grafted polymers act therefore as pressure patches applied to the surface. Although we only study here linear chains attached by one end, it is clear that modification of the polymer architecture opens the possibility of tailoring a diversity of pressure tools customized to particular applications. When the pressure patch is applied to a deformable surface, the ensuing deformation carries the signature of the non-homogeneous pressure field. We will present the characteristic pinched form of an elastic surface under the grafted polymer pressure. This deformation field is at the origin of the second important force at work here: membrane-mediated attraction or repulsion between patches is achieved when the chains are grafted, respectively, to the same or to opposite sides of the membrane.

We first consider a Gaussian polymer chain end-tethered to a flat surface. The interactions between the polymer and the surface are purely repulsive; the polymer concentration vanishes at the surface. The partition function for a terminally grafted polymer is [10]

$$Z(\mathbf{r};N) = \int d\mathbf{r}' \, G_N(\mathbf{r},\mathbf{r}'), \qquad (1)$$

where $G_N(\mathbf{r},\mathbf{r}')$, is the Green function of the Gaussian polymer. The integral runs over all the volume available to the free-end of the polymer; the grafted end is fixed at the origin of coordinates, at a monomer distance from the wall $\mathbf{r} \equiv (0,0,a)$. The Green function obeys the Edwards equation [10]

$$\frac{a^2}{6}\Delta_{\mathbf{r}} G_N(\mathbf{r},\mathbf{r}') = \frac{\partial G_N}{\partial N}(\mathbf{r},\mathbf{r}') \quad, \qquad (2)$$

with the following boundary conditions: $G_N(\mathbf{r},\mathbf{r}') = 0$ at the walls $\mathbf{r}_\perp = 0$, and $G_{N\to 0}(\mathbf{r},\mathbf{r}') = \delta(\mathbf{r}-\mathbf{r}')$. We now perform a virtual small displacement $\zeta(x,y)$ of the surface and perturbatively solve the Edwards equation with the new boundary coundition $G_N(\mathbf{r},\mathbf{r}') = 0$ at the wall position $\mathbf{r}_\perp = \zeta(x,y)$. This displacement can be achieved by the work

$$\Delta F = -K_B T \ln\left[\frac{Z(\zeta)}{Z(\zeta=0)}\right] = \int dxdy \, p(x,y)\zeta(x,y), \quad (3)$$

of the entropic pressure field $p(r=\sqrt{x^2+y^2})$ given by

$$p(r) = \frac{1}{2\pi}\frac{K_B T}{(r^2+a^2)^{3/2}}\left(1 + \frac{r^2+a^2}{2R_g^2}\right)\exp\left\{-\frac{r^2+a^2}{4R_g^2}\right\}, \qquad (4)$$

where K_B is the Boltzmann constant, T the absolute temperature, and $R_g^2 = Na^2/6$ is the typical size of a polymer with N monomers of length a. Figure 1 shows a plot of the pressure equation (4). Not surprisingly, the pressure patch has radial symmetry and its strength decays from the center as $p(r) \sim K_B T r^{-3}$, the natural scaling form for the pressure close to the grafting point $(a \ll r \ll R_g)$, where the only relevant length is r. At distances larger than the polymer size $(r \gg R_g)$ the pressure vanishes exponentially. Note the very high value of the pressure in the neighborhood of the graft-
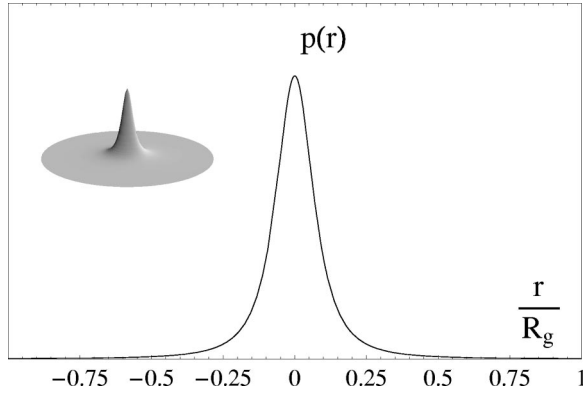
FIG. 1. The pressure applied by a grafted polymer to the surface. We chose here $a = 0.1 R_g$ and arbitrary units of pressure. The inset stresses the cylindrical symmetry of this particular pressure patch.

ing point $p(r=a) \simeq K_B T/(2\pi a^3) \simeq 2.4 \times 10^7$ Pa for $a = 3$ Å at room temperature $T = 25\,°C$. The area within a monomer distance from the grafting point supports indeed a finite fraction of the total force exerted by the polymer onto the surface, $f = \int_0^\infty 2\pi r p(r) dr \simeq K_B T/a = 13.3$ pN for the precedent values of monomer size and temperature.

The forces described above can be applied to a wide class of surfaces, provided that grafting of nonadsorbing chains is feasible. In membrane systems, grafting is easily achieved by using polymer chains that carry hydrophobic groups. Typical examples are provided by the so-called PEG-lipids, hydrophilic chains of polyethylene glycol covalently linked to a double-tail phospholipid molecule, or by Myrj 59, a polyethylene glycol chain attached to a stearate hydrophobic group. The hydrophobic moities mix well with the bilayers, effectively anchoring the polymer. For flaccid vesicles or dilute lamellae, in which the membranes are under a vanishing small-surface tension, only the curvature elastic rigidity will resist the polymer pressure. The deformation profile ζ is therefore a compromise between the applied pressure and the restoring forces of the bending elasticity, and it will minimize the functional form

$$F = \frac{k}{2} \int_0^\infty 2\pi r dr [\Delta_r \zeta(r)]^2 + \int_0^\infty 2\pi r p(r) \zeta(r) dr, \quad (5)$$

with $\Delta_r = (1/r)(d/dr)r(d/dr)$ the two-dimensional Laplacian operator and k the membrane elastic rigidity with dimensions of energy [11,12]. The resulting deformation (see Fig. 2) close to the center of the pressure patch has a cone shape

$$\zeta = -\frac{K_B T}{2\pi k} r, \quad r \to 0, \quad a = 0, \quad (6)$$

independent of the boundary conditions acting on the membrane. This is also the shape that one would find if a purely conic deformation of an arbitrary angle was allowed to relax under the attached polymer, as first noted in Ref. [13], a further confirmation that the central region carries most of the total stress imposed upon the interface. Note, however, that the conic form presented in Ref. [13] only coincidentally agrees with the central part of our profile. In fact, a prediction of the membrane shape requires the knowledge of the
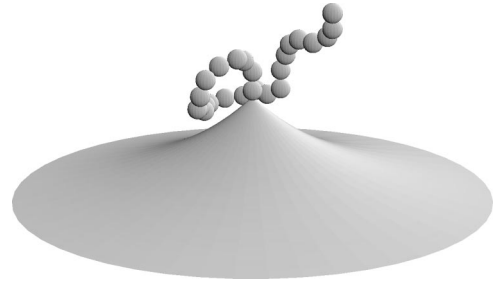

FIG. 2. The pinched form of an elastic membrane under the pressure of a grafted polymer. The deformation profile is the actual, calculated form but the polymer is only represented for clarity.

structure of the pressure field that has, as we have shown for grafted polymers, the dominant form $p(r) \sim r^{-3}$. In general, if one considers a general pressure field of the form $p(r) \sim r^{-m}$, the membrane will assume the shape $\zeta \sim r^{4-m}$. For free-standing membranes, the deformation field at distances larger than the polymer size is the catenoid shape, with zero average curvature.

We now display in Fig. 3 the deformations for supported membranes, an important pratical configuration. Here, the membrane adheres to a solid support with adhesive energy Γ. Application of the pressure patch peels a circular region of the membrane with radius L and central height $\zeta_0 = \zeta(r = 0)$. The central part of the pinched form is not changed by the boundary conditions where the elastic torque balances the adhesive forces that hold the membrane to the supporting surface: $\Delta \zeta(r=L) = \sqrt{\Gamma/k}$. The characteristic dimensions of the pinch, ζ_0 and L, depend on the dimensionless number $\beta = k\Gamma R_g^2/(K_B T)^2$. For small adhesive energies or very flexible membranes ($\beta \ll 1$) the membrane is only loosely attached to the surface and the deformation is similar to the free-standing case described above. For large adhesive energies or stiff membranes ($\beta \gg 1$), only the conic deformation survives and the peeled radius is proportional to the pinch height

$$L \simeq \frac{8}{3} \zeta_0 \simeq \frac{1}{2\pi} \frac{K_B T}{k} \sqrt{\frac{k}{\Gamma}} . \quad (7)$$

Typical adhesion energies [14,15] in the range $\Gamma \sim 10^{-7} - 10^{-4}$ mN m^{-1} and membrane rigidities $k \sim 5 - 20 K_B T$ [12] would lead to sizes of the peeled zones in the range of 1–10 nm, which is also the range where lie typical polymer sizes. Swollen vesicles, monolayers, and other interfaces un-
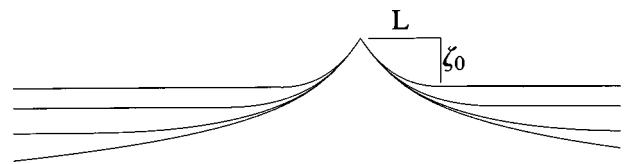

FIG. 3. The deformation profiles of a supported membrane holding a grafted polymer, for different adhesive strengths Γ (see text). The lower profile corrresponds to the free-standing case. Successive profiles from bottom to top scan increasingly larger values of Γ. Note that, as expected, the height of the deformation and the extension of the peeled zone decrease with Γ while the central region is not perturbed by the adhesive process.
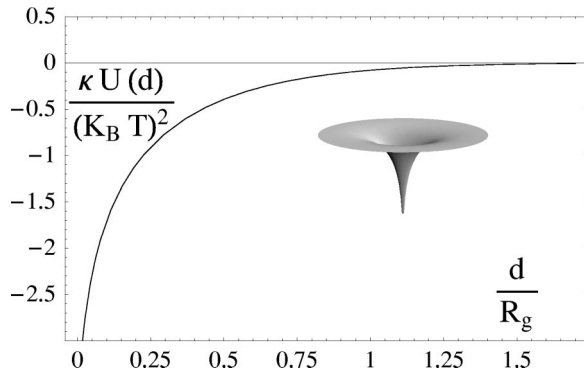
FIG. 4. The membrane-mediated interaction potential between two Gaussian polymers, grafted to the same side of a membrane with bending rigidity. Polymers grafted on opposite sides have the same functional form with the reverse sign.

der tension behave in a similar way. The distortion close to the grafting point is independent of the interfacial tension over a region proportional to $\sqrt{k/\Gamma}$, but details of the far field depend on boundary conditions. In particular, oscillating deformation profiles are generated in lamellar phases [16] where the membrane regions far from the center of pressure are held by a soft interlamellar potential rather than attached to a solid interface.

When two or more pressure patches are applied to a deformable interface, the possibility arises of interpatch interactions. The basic mechanism behind the interactions is deformation sharing. It is easier for a second polymer to reshape a membrane already deformed by a polymer grafted on the same side, leading to an attractive potential. Conversely, it is clear that two pressure patches applied on opposite sides of a membrane will mutually cancel the deformation, leading to repulsion. Within our framework, these attractive and repulsive potentials $U_{att}(d)$ and $U_{rep}(d)$ have the same functional dependence on the distance between anchoring points d, but opposite signs. The potential $U_{att}(d)$ displayed in Fig. 4 has, for short separation distances d, a logarithmic shape

$$U_{att}(d) = -U_{rep}(d) = \frac{(K_BT)^2}{2\pi k}\ln\frac{d}{R_g}; \quad d\to 0, \qquad (8)$$

and vanishes exponentially for distances larger than the polymer size R_g.

Taking into account membrane-mediated interaction forces is crucial for describing shape transformations in membrane systems. For instance, it is clear that attraction between different patches on the same side of the membrane will lead to a spontaneous local reinforcement of the deformation. Depending on the temperature and elastic constants, this process can eventually lead to the formation and extraction of small vesicles from the main membrane, a process known as budding [17]. Also, the strong temperature dependence of the interaction potential can explain the behavior of molecular accordions. Ringsdorf and collaborators [7,8] build such ''instruments'' by ornamenting liposomes with hydrophobically modified, water-soluble polymers. Due to the presence of hydrophobic groups along the backbone, the polymer makes several loops at the liposome surface. An increase of the temperature leads to the aggregation of the anchoring points—monitored by a variation of fluorescent activity of the labeled hydropobic moities—a process that can be reversed by consecutively lowering the temperature. The authors interpreted this accordion cycle by invoking polymer collapse in poor solvent conditions, but the interplay of the attractive forces described above and the excluded volume interactions between loops would also lead to the same interesting behavior.

Results presented in this paper only refer to Gaussian chains. In most solvents, the chains do not follow random walk statistics, but excluded volume interactions need instead to be considered. The scaling argument for the pressure $p(r)\sim K_BT/(r={}$only relevant length$)^3$ suggests that the r^{-3} scaling behavior should persist for chains with excluded volume, a result consistent with our preliminary results of work under progress on Monte Carlo simulations of grafted self-avoiding walks.

The pinched forms displayed in Figs. 2 and 3 are a direct result of the nonhomogeneity of the pressure applied by the polymer to the membrane. Different degrees of homogeneity, and therefore different induced deformations, can be conceived by considering chain architecture, electrostatic interactions, and solvent quality. For instance, by connecting several grafted polymers in a larger comblike molecule, it is possible to break the local cylindrical symmetry of the patch. Combination of polymers and rigid colloidal particles leads to entropic forces acting only in specific regions determined by colloid geometry. If the polymer is charged, other effects also come into play. Even at neutral interfaces, a charged polymer is repelled from the surface by its image charge, resulting in a reduction of the applied entropic pressure. The Maxwell pressure [18], which originates on the distortion of the electric field by the dielectric discontinuity, also acts as a surface patch. The strength of a ''Maxwell patch'' will in general have a functional form different from the entropic patches considered here. Combination of both entropic and electrostatic pressures further enhances the possibility of designing customized mesoscopic force tools, suitable for each given application.

Note added in proof. Some results described here have recently been published in an independent work by Breidenich, Netz, and Lipowsky [19].

[1] B. Alberts, *Molecular Biology of the Cell* (Garland, New York, 1994).

[2] J. van de Pas *et al.*, Colloids Surf., A **85**, 221 (1994).

[3] H. Warriner *et al.*, Science **271**, 969 (1996).

[4] Y. Yang *et al.*, Phys. Rev. Lett. **80**, 2729 (1998).

[5] G. Bouglet and C. Ligoure, Eur. Phys. J. B **9**, 137 (1999).

[6] R. Joannic, L. Auvray, and D.D. Lasic, Phys. Rev. Lett. **78**, 3402 (1997).

[7] H. Ringsdorf, J. Venzmer, and F. Winnik, Angew. Chem. Int. Ed. Engl. **30**, 315 (1991).

[8] M. E. Cates, Nature (London) **351**, 102 (1991).

[9] V. Frette *et al.*, Phys. Rev. Lett. **83**, 2465 (1996).

[10] M. Doi and S. F. Edwards, *The Theory of Polymer Dynamics* (Clarendon Press, Oxford, 1986).

[11] W. Helfrich, Z. Naturforsch. A **28c**, 693 (1973).

[12] S. Safran, *Statistical Thermodynamics of Surfaces, Interfaces and Membranes* (Addison-Wesley, Reading, MA, 1994).

[13] R. Lipowsky, Europhys. Lett. **30**, 197 (1995).

[14] A. Albersdörfer, R. Bruinsma, and E. Sakmann, Europhys. Lett. **42**, 227 (1998).

[15] U. Seifert and R. Lipowsky, Phys. Rev. A **42**, 4768 (1990).

[16] T. Bickel, C. M. Marques, and C. Jeppesen (unpublished).

[17] Y. Kim and W. Sung, Europhys. Lett. **47**, 292 (1999).

[18] L. D. Landau, E. Lifshitz, and L. P. Pitaecskii, *Electrodynamics of Continuous Media* (Butterworth-Heinemann, Oxford, England, 1995).

[19] M. Breidenich, R. R. Netz, and R. Lipowsky, Europhys. Lett. **49**, 431 (2000).